Human Molecular Genetics, 2001, Vol. 10, No. 8 797–806

Functional hemizygosity of PAFAH1B3 due to a *PAFAH1B3–CLK2* fusion gene in a female with mental retardation, ataxia and atrophy of the brain

Hans Gerd Nothwang[1,2], H.G. Kim[1], J. Aoki[3], M. Geisterfer[4], S. Kübart[1], R. D. Wegner[5], A. van Moers[5], L. K. Ashworth[6], T. Haaf[1], J. Bell[4], H. Arai[3], N. Tommerup[7], H. H. Ropers[1,8,+] and J. Wirth[1]

[1]Max-Planck-Institut für Molekulare Genetik, Ihnestrasse 73, D-14195 Berlin-Dahlem, Germany, [2]FB Biologie, Universität Kaiserslautern, Kaiserslautern, Germany, [3]Department of Health Chemistry, University of Tokyo, Japan, [4]Ottawa Regional Cancer Centre, Ottawa, Canada, [5]Institut für Humangenetik, Freie Universität Berlin, Berlin, Germany, [6]Lawrence Livermore National Laboratory, Livermore, CA, USA, [7]Department of Medical Genetics, IMBG, Copenhagen, Denmark and [8]Department of Human Genetics, University Hospital, Nijmegen, The Netherlands

Received 30 October 2000; Revised and Accepted 15 February 2001

We report on the molecular characterization of a translocation t(1;19)(q21.3;q13.2) in a female with mental retardation, ataxia and atrophy of the brain. Sequence analysis of the breakpoints revealed an *Alu*-repeat-mediated mechanism of recombination that led to truncation of two genes: the kinase *CLK2* and *PAFAH1B3*, the gene product of which interacts with LIS1 as part of a heterotrimeric G protein complex PAF–AH1B. In addition, two reciprocal fusion genes are present. One expressed fusion gene encodes the first 136 amino acids of PAFAH1B3 followed by the complete CLK2 protein. Truncated PAFAH1B3 protein lost its potential to interact with LIS1 whereas CLK2 activity was conserved within the fusion protein. These data emphasize the importance of PAF–AH1B in brain development and functioning and demonstrate the first fusion gene apparently not associated with cancer.

INTRODUCTION

Approximately 2–3% of the human population present with mental retardation (MR, IQ < 70) and it is estimated that 5–10% of mild MR (IQ 50–70) and ~50% of severe MR (IQ < 35) have a genetic cause (1). Several genes for X-linked MR have been recently isolated, but elucidation of the molecular defects underlying autosomal MR remains a major challenge. This is due to the enormous genetic heterogeneity as demonstrated by the analysis of X-linked forms (1). This hampers the efficient identification of autosomal candidate genes by genome-wide linkage analysis, since most families are too small and their data cannot be combined with those of other families. A suitable approach to overcome this problem is the characterization of chromosomal rearrangements associated with MR. This method has already been instrumental in the positional cloning of several MR disease genes and is further supported by several studies that indicate an increase of balanced structural rearrangements among the retarded (1–4).

To fully exploit the information provided by MR associated chromosome rearrangements, the Mendelian Cytogenetic Network (MCN) has identified more than 1000 such cases (N. Tommerup, unpublished data). In addition, a comprehensive YAC panel over the entire human genome was recently established (5) and this tool, together with the rapidly progressing sequence information of the human genome, allows the characterization of these rearrangements with reasonable effort. Therefore, we initiated a systematic analysis of *de novo* balanced chromosomal rearrangements associated with any kind of MR.

Here, we report on a proband with brain dysfunction and dysmorphology, and a translocation t(1;19)(q21.3;q13.2). Molecular characterization of this translocation revealed a complex genotype with the truncation of two genes and the formation of two reciprocal fusion genes. Both breakpoints were characterized in detail to unravel the mechanism of the non-homologous rearrangement between chromosomes 1q21.3 and 19q13.2. Furthermore, the major fusion protein was functionally analysed.

RESULTS

Delineation of the breakpoint regions on 1q21.3 and 19q13.2

A female patient was reported with MR, ataxia and atrophy of the brain. Cytogenetic analysis revealed an apparently balanced *de novo* translocation t(1;19)(q21.3;q13.2). Fluorescence *in situ* hybridization (FISH) analysis of mega-YAC clones from a genome-wide YAC panel narrowed down the breakpoints on both chromosomes to intervals of <3 cM. YAC clone CEPHy904F05930 containing STS D1S2771 (173 cM)

[+]To whom correspondence should be addressed at: Max-Planck-Institut für Molekulare Genetik, Ihnestrasse 73, D-14195 Berlin-Dahlem, Germany; Tel: +49 30 8413 1240; Fax: +49 30 8413 1383; Email: ropers@molgen.mpg.de

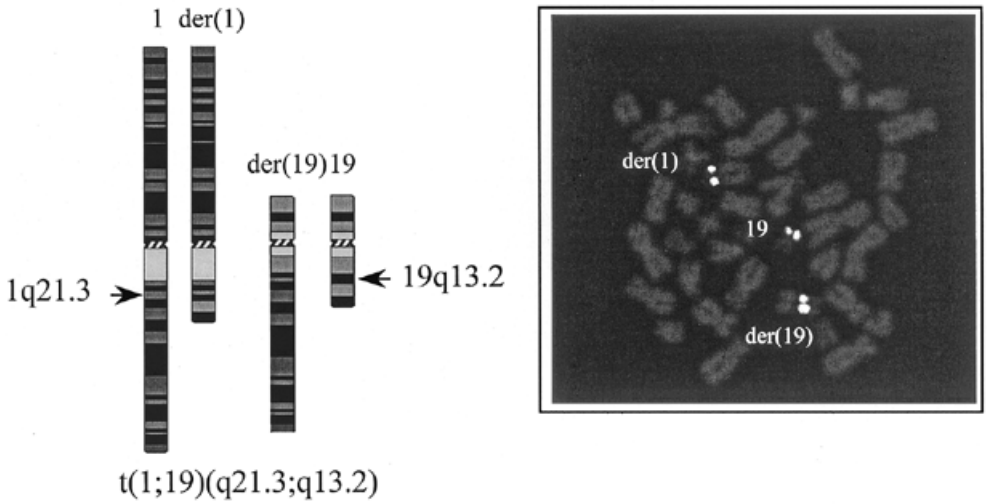

Figure 1. FISH analysis of t(1;19)(q12;q13.2). (**A**) Ideogram of the chromosomes, involved in the translocation of patient E.B., with arrows at the breakpoint positions. (**B**) FISH of cosmid F19975 to metaphase spreads of patient E.B. The cosmid clone spans the breakpoint since its hybridization signal is seen on the normal chromosome 19 and the derivative chromosomes 1 and 19 [der (1) and der (19)].

mapped proximal and clone CEPHy904D05873 containing STS D1S484 (174 cM) distal to the breakpoint on 1q21.3. The breakpoint on chromosome 19 was located between markers D19S223 (64 cM) and D19S420 (66 cM), since YAC clones CEPHyC10875 and CEPHy904C01761 mapped proximally and distally, respectively, to the breakpoint (data not shown). Since chromosome 19 is well covered by ordered genomic clones (6), the 19q13 breakpoint was cytogenetically and molecularly characterized in more detail. For high-resolution mapping, cosmid clones from a chromosome 19 contig in this region were analysed by FISH. Two clones, F19975 and R31213, hybridized to the normal chromosome 19, to der(1) and to der(19), and thus spanned the breakpoint on 19q13.2 (Fig. 1). The localization of the breakpoint was confirmed by cosmids that physically had been mapped adjacent to these cosmids: cosmid R34603 mapped proximally and cosmid R27716 distally to the breakpoint according to FISH results (data not shown).

PAFAH1B3 on 19q13.2 is truncated by the translocation

The restriction patterns of the breakpoint spanning cosmids demonstrated overlap with the sequenced BAC clone CIT-B-147B23 (GenBank accession no. AC006486) (data not shown). Sequence analysis identified two genes in the breakpoint area: *KIAA0306* and *PAFAH1B3* (GenBank accession nos AB002304 and D63391). Southern blot hybridization with EST clones corresponding to *KIAA0306* did not detect aberrant bands in patient DNA compared with a control DNA (data not shown). Hybridization of cDNA clones corresponding to *PAFAH1B3*, however, resulted in the detection of several additional fragments in restricted patient DNA (data not shown). A comparison of the hybridization signals with the restriction pattern, obtained by *in silico* analysis of the sequence, suggested that the breakpoint is located between exons 4 and 5 of *PAFAH1B3*. To confirm this localization, a 3 kb *Rsa*I fragment of the intron 4 region was amplified by PCR and probed on a Southern blot. Again, it detected additional fragments in patient DNA restricted with four different enzymes: 6 kb and ~13 kb (*Ecl*136II), >23 kb (*Eco*RV), 3.5 kb (*Dra*I) and 1.1 kb (*Rsa*I) (Fig. 2). Thus, the gene *PAFAH1B3* is disrupted between exons 4 and 5 by the translocation on chromosome 19q13.2. The encoded protein forms with two other subunits the platelet-activating factor (PAF) acetylhydrolase 1B (PAF–AH1B) complex and bears the hydrolytic activity of this enzyme that produces biologically inactive lyso-PAF (1-*O*-alkyl-2-hydroxy-*sn*-glycero-3-phosphocholine) (7). The disruption leads to a truncated allele that encodes a protein with only the first 136 instead of 232 amino acid residues, lacking amino acids Asp192 and His195 (8). Together with Ser47, these two amino acids form the catalytic triad and their substitution leads to loss of hydrolytic activity (8).

A second gene, *CLK2* on 1q12.3, is disrupted

To characterize the breakpoint on chromosome 1, the junction fragment was cloned by genome walking. *Rsa*I-restricted genomic DNA from the patient was ligated to an adaptor, and nested PCR using adapter- and chromosome 19-specific primers was performed. Human primers were derived from the breakpoint-spanning 3 kb *Rsa*I fragment of *PAFAH1B3* intron 4. This PCR yielded a product of ~1.1 kb (data not shown). This size corresponded well with that of the aberrant *Rsa*I fragment seen in the patient lane on the Southern blot (Fig. 2). Sequence analysis of this junction fragment demonstrated identity both to BAC clone CIT-B-147B23 on chromosome 19 and to a sequence on chromosome 1q21 that contains several genes (GenBank accession no. AF023268) (9).

The breakpoint on chromosome 19 is situated between nucleotides 91 425 and 91 426 of BAC clone CIT-B-147B23 and between nucleotides 606 and 607 of the genomic sequence on chromosome 1. These data revealed that a second gene, the dual specificity *cdc-like kinase 2* (*CLK2*) on 1q21, is disrupted (Fig. 3) (10,11). The first nucleotide of *CLK2* corresponds to

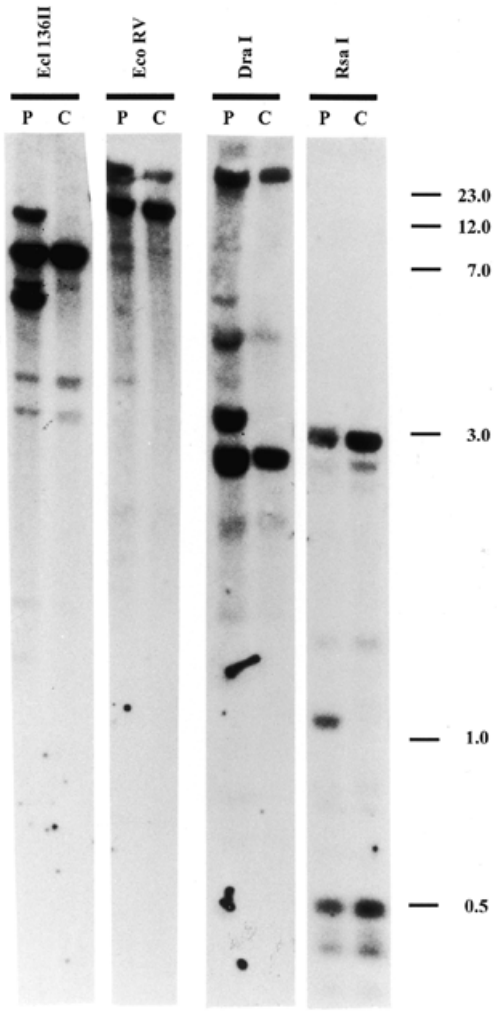

Figure 2. Disruption of *PAFAH1B3* by t(1;19). Hybridization of an [α-^{32}P]dCTP-labelled *PAFAH1B3* intron 4 sequence to a Southern blot containing restricted DNA from the patient (P) and from a control (C). Novel aberrant restriction fragments are seen in DNA from the patient restricted with the enzymes indicated. DNA size is shown to the right in kb.

the first nucleotide of the reported genomic sequence and the gene terminates at nucleotide 10 482 of the genomic sequence. Exon 1 encompasses nucleotides 1–129 and exon 2 nucleotides 2354–2523 of the published genomic sequence. Thus, the breakpoint between nucleotides 606 and 607 is situated in intron 1 and separates exon 1, containing the 5′untranslated region (UTR) from exon 2 that starts directly with the ATG initiation codon. The open reading frame (ORF) of *CLK2* is therefore not disrupted (Fig. 3).

Expression of the fusion gene *PAFAH1B3Δex5–CLK2Δex1*

According to sequence analysis, two fusion genes are present: on der(19), *CLK2* exon 1, which contains the complete 5′ UTR is fused to exon 5 of *PAFAH1B3*, which encodes the final 95 amino acids and harbours the 3′ UTR, and on der(1), exons 2–13 of *CLK2* are fused to exons 1–4 of *PAFAH1B3*, resulting in a large fusion gene, *PAFAH1B3Δex5–CLK2Δex1* (Fig. 3). The latter will give rise to a protein containing amino acids 1–136 of PAFAH1B3, followed by the complete and unmodified CLK2 polypeptide, since exon 2 of *CLK2*, starting with the initiation codon ATG, is fused in frame to *PAFAH1B3*. The small fusion gene *CLK2Δex2-13–PAFAH1B3Δex1-4* on der(19) might be translated into a 42 amino acid long polypeptide, since there is an ATG codon in exon 5 at position 681 of *PAFAH1B3*, situated within a potential Kozak consensus sequence (**GACATG**) (12).

To corroborate this *in silico* analysis and to demonstrate the expression of the large fusion gene *PAFAH1B3Δex5–CLK2Δex1*, RT–PCR analysis was performed with *PAFAH1B3*-derived forward and *CLK2*-derived reverse primers. A 2.2 kb RT–PCR product could be amplified from an mRNA population that was isolated from a lymphoblastoid cell line of the patient. No cDNA could be amplified using a reverse transcribed control RNA (Fig. 4). The size of 2.2 kb corresponded well with the predicted 2242 nucleotides of the fusion transcript and sequence analysis confirmed that this cDNA product represented the fusion gene (data not shown).

No mutation in the intact alleles of *PAFAH1B3* and *CLK2*

The disruption of a gene by a balanced translocation might render a recessive mutation on the other allele homozygous. To determine whether the intact *CLK2* and/or *PAFAH1B3* alleles bear point mutations, both mRNAs were reverse transcribed, amplified and sequenced. To analyse only transcripts derived from the non-disrupted alleles, PCR primers were derived from exons 1 and 13 for *CLK2*, and from exons 1 and 5 for *PAFAH1B3*. No mutation was found, arguing against an unmasking of heterozygosity by the translocation (data not shown).

Loss of function of PAFAH1B3 and conservation of function of CLK2 in the fusion gene

To dissect the contribution of the two truncated genes to the phenotype, the function of their encoded proteins within the fusion product was analysed. PAFAH1B3 is part of a G-protein-like heterotrimer and interacts with one of the other two subunits, LIS1. To test the interaction of the fusion protein with LIS1, we used the yeast two-hybrid system with GAL4. This molecular genetic analysis demonstrated that the interaction between the truncated PAFAH1B3 within the fusion protein and LIS1 is impaired (Fig. 5). Only wild-type PAFAH1B3 binds to LIS1, but not the fusion protein (Fig. 5A), since only co-transfection of *PAFAH1B3* and *LIS1* leads to yeast growth on selection media.

The *CLK2* gene product was previously shown to co-localize with splicing factors and to regulate the alternative splicing of a model precursor mRNA (11). To assess the function of CLK2 in the fusion protein, we studied the reported regulatory activity on splicing and the subcellular localization (11). For the latter, the fusion gene was subcloned into a GFP-vector and subcellular distribution of the encoded fusion protein was compared with wild-type Clk2–GFP fusion protein after transfection into COS1 cells. No differences could be detected (Fig. 6A). Functional analysis had demonstrated that CLK2 is involved in the regulation of pre-mRNA splicing. To assess this activity, the fusion gene was co-transfected with a *Clk1* minigene (13). Increasing amounts of the fusion gene trans-

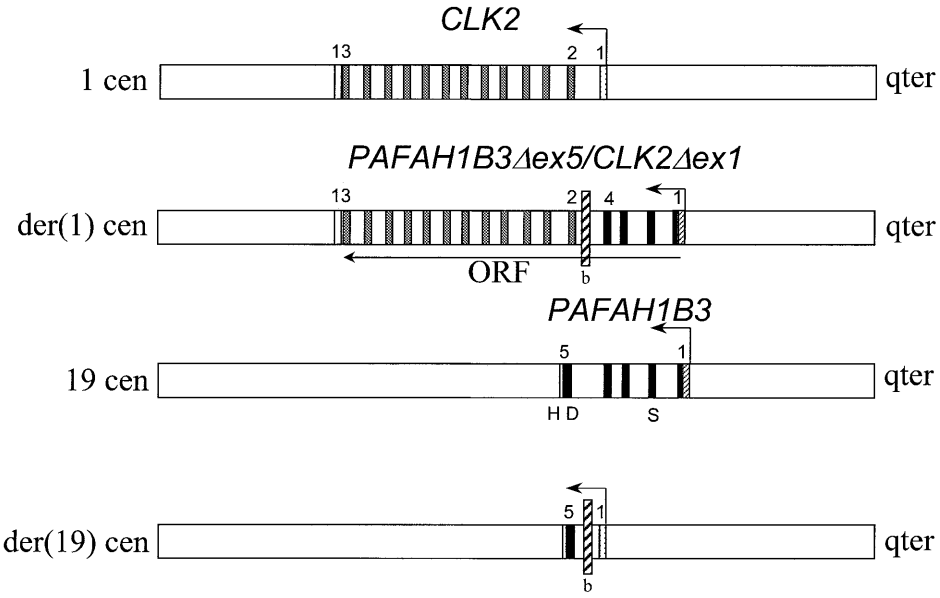

Figure 3. Gene structure of *PAFAH1B3*, *CLK2* and the fusion genes caused by t(1;19). Schematic representation of chromosomes 1, 19, der(1) and der(19) at the breakpoint regions. The affected genes *CLK2* and *PAFAH1B3* are indicated with their gene structure. Filled bars represent coding regions, punctuated bars 5′ UTR of *CLK2*, hatched bars 5′ UTR of *PAFAH1B3*, unfilled bars untranslated 3′ UTR regions, important exons are numbered. The direction of gene transcription is indicated by arrows and the breakpoints by hatched boxes, ORF, open reading frame; b, breakpoint. Note that exon 2 of *CLK2* starts with the initiation codon ATG that is fused in frame to *PAFAH1B3Δex5* on der (19).

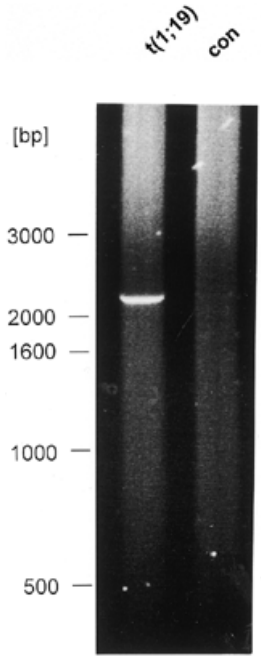

Figure 4. Expression of the fusion gene *PAFAH1B3Δex5–CLK2Δex1*. Nested RT–PCR was performed by using forward primers in exon 1 of *PAFAH1B3* and reverse primers in exon 13 of *CLK2*. Reverse transcribed patient RNA [t(1;19)], but not RNA from a normal individual (con), resulted in amplification of a fusion transcript of the expected size of 2.2 kb. The amplified fusion gene from the patient was confirmed by sequence analysis.

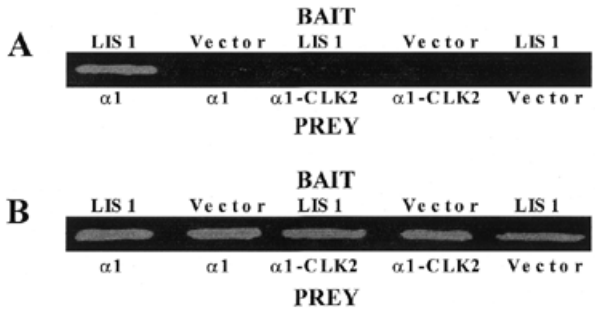

Figure 5. Lack of interaction between the fusion gene and LIS1 in a yeast two-hybrid assay. HF7c yeast cells were cotransformed with a 'bait' vector and a 'prey' as indicated. Cotransformation efficiency was determined by their ability to grow on selection media lacking leucine and tryptophan as shown in (**B**). Binding between the bait fusion protein and the prey fusion protein was assayed by nutritional selection on histidine-dropout media (**A**). α1 refers to PAFAH1B3.

fected per cell promoted exon skipping in the *Clk1* pre-mRNA *in vivo* to the same degree as transfection of similar amounts of *Clk2* (Fig. 6B and C). These analyses suggest that functional hemizygosity of PAFAH1B3 contributes to the phenotype (see Discussion).

Alu repeat element-mediated recombination between 1q21.3 and 19q13.2

Knowing the sequences of both breakpoint regions, it was of interest to analyse the molecular basis of the recombination between non-homologous chromosomes. Sequence analysis revealed the presence of *Alu* repetitive elements in both breakpoint regions (Fig. 7A). The breakpoint on chromosome 1 is situated in the so-called B sequence of the left arm between nucleotides –90 and –88 of the *Alu*Sp consensus sequence. The B sequence is part of a bipartite structure (block A and block B) that is homologous to the internal promoter of genes transcribed by polymerase III and that is essential for *Alu* repeat transcription (14). The breakpoint on chromosome 19 is localized between nucleotides –23 and –25 of the right arm of the *Alu*Y

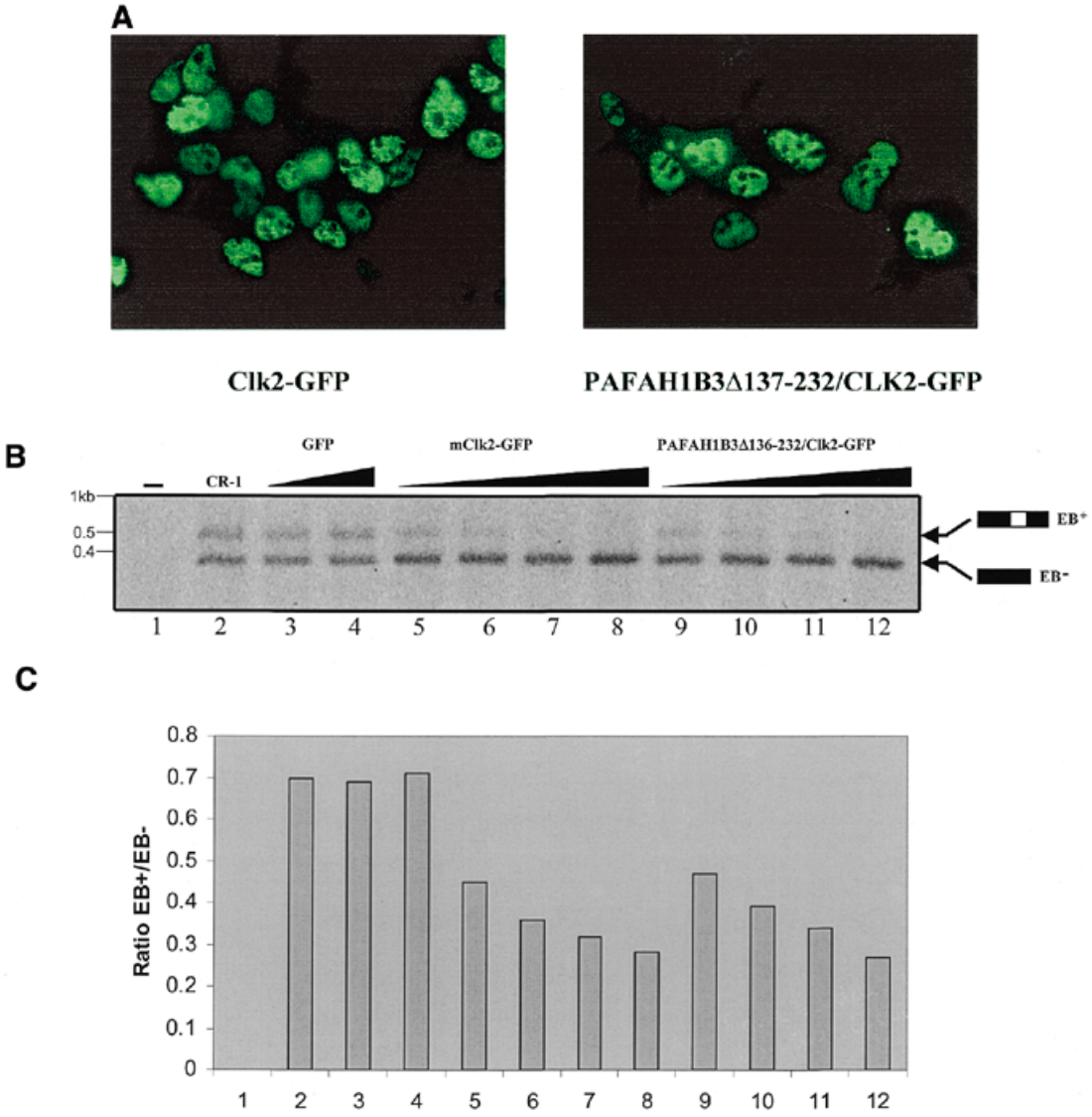

Figure 6. CLK2 is functional in the fusion protein PAFAH1B3–CLK2. (**A**) GFP fusion constructs were transfected into COS-1 and subcellular localization determined by fluorescence microscopy. (**B**) Pattern of Clk1 alternative splicing upon transfection of pEGFPN1-*Clk2* or pEGFPN1- *PAFAH1B3Δex5–CLK2Δex1*. Lane 1, cells with filler DNA; lane 2, 1 µg CMV-*Clk1* minigene; lanes 3–12, 1 µg CMV-*Clk1* minigene plus 0.1 and 0.5 µg pEGFP-N1 vector (lanes 3 and 4), 0.01, 0.05,0.1 and 0.5 µg pEGFPN1-*Clk2* (lanes 5–8) or 0.01, 0.05, 0.1 and 0.5 µg pEGFPN1-*PAFAH1B3Δex5–CLK2Δex1* (lanes 9–12), respectively. (**C**) Ratios for *Clk1* mRNAs.

consensus sequence. The breakpoints in these two parallel-orientated *Alu*-elements are located in non-homologous nucleotide stretches, as shown by the alignment (Fig. 7B). Interestingly, on chromosome 19, an *Alu*SP repeat element is only 14 bp away from the *Alu*Y element that would have allowed a perfect alignment with the *Alu*Sp element on chromosome 1 (Fig. 7A).

DISCUSSION

The molecular characterization of a translocation between 1q21.3 and 19q13.2 in a patient with brain dysfunction revealed that two genes, *PAFAHA1B3* and *CLK2*, are disrupted. PAFAH1B3 is a protein with similarity to p21ras and other GTPases and represents the α1 subunit of the PAF–AH1B complex that is a G-protein-like (α1,α2)β trimer and inactivates PAF (8,15). PAF is a potent phospholipid messenger molecule, implicated in a variety of physiological events (see below). CLK2 is a ubiquitously expressed cdc-like protein kinase that phosphorylates serine/threonine as well as tyrosine. It regulates the distribution of the serine/arginine-rich (SR) family of splicing factors (10,11). In addition, the fusion gene *PAFAH1B3Δex5–CLK2Δex1* is expressed. To our knowledge, this is the first report on a human fusion gene apparently not associated with cancer, since the patient so far does not present any sign of tumour. Up to now, fusion genes have been only reported from studies of tumour type-specific chromosome translocations like the *BCR–ABL* fusion in the Philadelphia chromosome (16).

Due to the complex genotype in the proband, several non-mutually exclusive mechanisms are possible to explain the

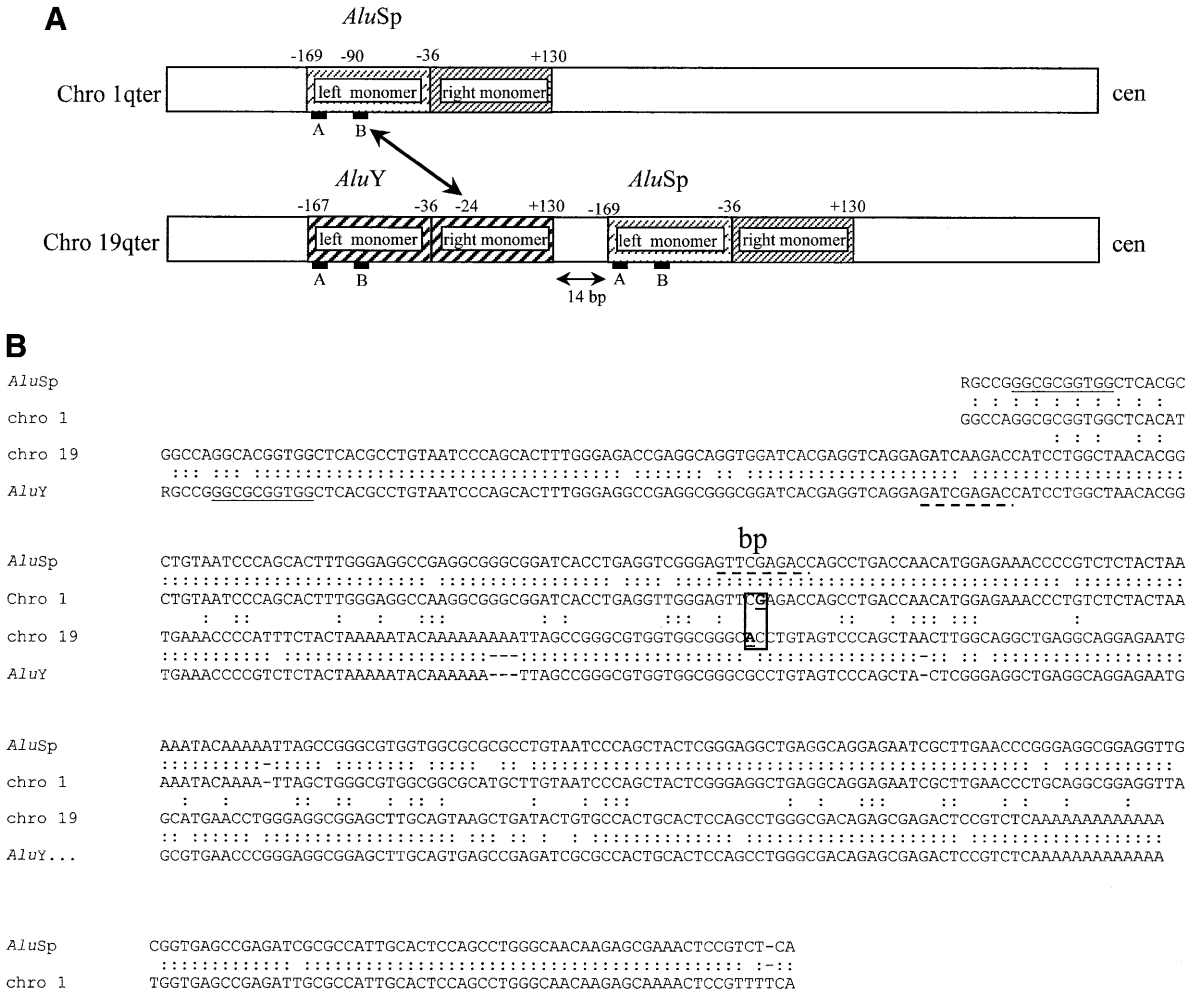

Figure 7. *Alu* repeat-mediated recombination. (**A**) Orientation of the relevant *Alu* repetitive sequences in the breakpoint regions on chromosome 1 and 19 are shown with their left and right monomers. The nucleotide numbering scheme is the same as described by Deininger *et al.* (42). Position +1 refers to the C of the *Alu* I endonuclease recognition site, AGCT. The bipartite promoter sequences A and B of the left monomer are indicated below the *Alu* repeats. An arrow points to the breakpoints of the rearrangement. (**B**) Sequence alignment of the junction fragment with the respective *Alu* repeats. The junction sequence is composed of chromosome 19 (before the breakpoint) and chromosome 1 sequences (after the breakpoint). Gaps are introduced to obtain optimum alignments and sequences were aligned to the (+) strand of the *Alu* repeat consensus sequences. Horizontal lines mark box A and dashed lines box B of the bipartite *Alu* promoter structure. The breakpoint (bp) is indicated by a box with the two nucleotides fused underlined.

phenotype. The most likely are: (i) truncation of *PAFAH1B3*; (ii) truncation of *CLK2*; (iii) a dominant effect of the fusion gene *PAFAH1B3Δex5–CLK2Δex1*; and (iv) unmasking of heterozygosity by the observed gene truncations. The latter is excluded by our analysis, since the intact alleles of *CLK2* and *PAFAH1B3* are expressed and bear no mutations. In analogy to tumour development, an attractive hypothesis is a gain-of-function of the encoded PAFAH1B3–CLK2 fusion protein in the patient. Many tumour-specific chromosomal rearrangements produce chimeric proteins that combine functions of the involved proteins in a way that leads to uncontrolled cell proliferation (16). Thus, an altered expression of *CLK2* in the fusion gene under the control of the *PAFAH1B3* promoter might contribute to the phenotype. This would explain why an intensive search in the OMIM and the MCN database as well as in the literature did not indicate any genetic disorder that is closely linked to either of the two breakpoint regions and that displays a similar phenotype and dominant mode of inheritance. However, the expression patterns of both genes, *PAFAH1B3* and *CLK2*, as judged by northern blot and EST database analysis, do not reveal a striking difference, e.g. both genes are expressed in the brain (10,17,18). We therefore favour a contribution of the *PAFAH1B3* gene truncation to the observed phenotype for reasons outlined below.

First, the observed truncation of *PAFAH1B3* leads to a functionally inactive protein since it cannot interact with LIS1. Furthermore, the truncated protein lacks the amino acids Asp192 and His195, essential for hydrolytic activity (8). These results clearly demonstrate functional hemizygosity for PAFAH1B3 in the patient. The truncated *CLK2*, in contrast, still contains an intact ORF and the encoded protein conserved its cellular activity within the fusion protein.

Second, RNA *in situ* hybridization analysis showed that PAFAH1B3 expression is developmentally regulated in most

brain regions and correlates with the period of neuronal migration in the cerebellum (17). These data indicate that despite its widespread expression in many tissues, PAFAH1B3 plays an important role during brain development. Third, a defect in the *PAFAH1B1* (= *LIS1*) gene, encoding a PAFAH1B3 interacting protein, causes MDLS (19), an autosomal dominant developmental disorder of the human brain manifested by severe retardation, poor control of movement, seizures, abnormal neuronal migration, thickened cortex with four rather than six layers and a smooth brain without convolutions or gyri. Several symptoms are thus similar to the reported phenotype of proband E.B., i.e. MR, seizures and impaired control of movements. These clinical features of proband E.B. as well as the atrophy of the brain would conform to a neuronal migration defect as is the case in MDLS. In addition, the dominant mode of inheritance of MDLS would fit with a dominant effect of PAFAH1B3 functional hemizygosity.

However, LIS1 also possesses physiological roles outside the PAF–AH1B complex. Solitaire LIS1 was shown to interact with doublecortin, tubulin and subunits of dynein and microtubules, and disturbance of any of these interactions might contribute to the LIS1 phenotype (20–27). For instance, mutations in the X-linked *DCX* gene result also in lissencephaly in males whereas females present with subcortical laminar heterotopia (28,29). This raises the question of whether PAF–AH1B plays a role at all in the pathogenesis of lissencephaly. Our finding of functional hemizygosity of another PAF–AH1B subunit, PAFAH1B3, in a patient with a neurological disorder indicates that PAF–AH1B does indeed play an important role in normal brain development and functioning. However, further mutations in independent patients will be necessary to clarify the precise relationship between PAF–AH1B3 and neurological disorders. Unfortunately, there are no candidate families available yet for mutation analysis.

An important role of PAF–AH1B in accurate brain development is also suggested by experiments showing that increased doses of PAF induce neuronal growth cone collapse and neurite retraction (30–32). In addition, PAF was shown to be involved in hippocampal long-term potentiation, a process associated with memory formation. Kato *et al.* (33) demonstrated that PAF served as a component in the biochemical events that modify the release of excitatory neurotransmitter during LTP.

The less severe phenotype in the patient reported here compared with lissencephaly might be explained by the additional functions of LIS1 outside the PAF–AH1B complex. Furthermore, northern blot and RNA *in situ* studies suggest that the oligomeric structure of PAF–AH1B is different from tissue to tissue since a differential expression of *PAFAH1B2* and *PAFAH1B3* was observed in various human tissues (17,18). It was therefore assumed that in some tissues, PAF–AH1B activity is formed by the subunits LIS1 and PAFAH1B2 that also bear catalytic activity (18).

The breakpoints on both chromosomes are located in *Alu* repetitive elements. *Alu*-mediated recombination is also the cause of the most common recurrent non-Robertsonian constitutional translocation in man between chromosomes 11q23 and 22q11 (34). Most *Alu*-mediated chromosome rearrangements involve the left monomer as with most rearrangements in the low density lipoprotein (LDL) receptor (35). It was suggested to be a hot spot of recombination due to the presence of a split polymerase III promoter, the transcription of which might induce a configuration prone to recombination (35). The breakpoint on chromosome 1 supports this idea since it is located in the B sequence of the left monomer like breakpoints reported in a human sex chromosome rearrangement and an adenosine deaminase deletion (reviewed in 36). The other breakpoint, on chromosome 19, departs, however, from this trend since it is localized in the right monomer as with several breakpoints in the gene *C1-INH*, encoding the plasma protein C1-inhibitor (36). It is of interest to note that even though both *Alu* repeats are orientated in parallel, the recombination took place in two non-homologous sequences. Furthermore, another *Alu*Sp repeat element in the same orientation is close to the *Alu*Y repeat on chromosome 19, which would have allowed a perfect homologous recombination. This suggests that there is an influence of flanking sequences or DNA conformation signals on the recombination.

In conclusion, the detailed characterization of the translocation revealed a rather complex genotype with two truncated genes and two fusion genes. This demonstrates that in studies of chromosomal rearrangements, both breakpoint regions have to be carefully analysed for the presence of genes. The functional hemizygosity of PAFAH1B3 in the patient strengthens the idea that PAF–AH1B plays a crucial role in brain function.

MATERIALS AND METHODS

Case report

The proband was born in 1973 to a 21-year-old mother and a 24-year-old father. She was the only child of healthy non-consanguineous parents. She was born at term by normal vaginal delivery after an uncomplicated pregnancy. Birth weight was 3150 g, length 51 cm and head circumference is not known.

At her first paediatric examination, coloboma of the left iris and congenital clubfeet were noted. The foot deformities were successfully treated by splints. An alternating convergent squint was apparent at 12 months. Motor developmental delay was evident in the early stages of life: her first independent steps were at 30 months, i.e. she walked with a broad based and stiff-legged gait. Fine motor skills were impaired; she displayed clumsy hand movements. Muscle weakness was not present and deep tendon reflexes were normal. Speech development was apparently delayed: first words were at 2.5 years and vocabulary and syntactic skills remained remarkably impaired. Formal IQ testing revealed impaired intellectual skills with a discrepancy between verbal and performance IQ (verbal IQ of 47, performance IQ of 71, mean IQ of 59). During early infancy she started to present introverted and auto-aggressive behaviour.

By the age of 4, the proband began having nocturnal generalized seizures, which could be controlled with valproate. Electroencephalography revealed multifocal spikes and sharp wave discharges. CT scans of the brain demonstrated slight cortical and subcortical asymmetric atrophy of the brain. However, the quality of the CT scan in 1979 did not allow for focal abnormalities of migration or leukencephalopathy. The mother did not consent to cranial MRI.

Cytogenetic studies

Chromosomal analysis was done on whole-blood cultures according to standard methods. To obtain prometaphase

chromosomes, the cultures were treated with methotrexate (0.05 µg/ml) after 48 h of incubation; bromodeoxyuridine (20 µg/ml) and fluorodeoxyuridine (1µg/ml) were added 6.5–7 h before being harvested. RBA-, GTG-, QFQ-, CBG-, DA-DAPI-banding of 250 metaphases of the proband and her parents were performed. The proband revealed a female karyotype with a *de novo* balanced reciprocal translocation between the long arm of chromosomes 1 and 19 with the karyotype: 46,XX,t(1;19)(q21.3;q13.2)

FISH

Standard FISH protocols were followed (37). DOP–PCR products of PFGE-purified YAC inserts or total cosmid DNA were labeled with either biotin-16-dUTP or digoxigenin-11-dUTP (Boehringer Mannheim) by using standard nick translation procedures. Metaphase spreads were prepared using standard procedures. Hybridization was done for 45 h in a moist chamber at 37°C. Immunocytochemical detection of the hybridization probes was achieved as described (5). Images were taken with a Zeiss epifluorescence microscope equipped with a thermoelectronically cooled charge coupled device (CCD) camera (Photometrics CH250), which was controlled by an Apple Macintosh computer. Merging and pseudo-coloring were accomplished using the ONCOR Image and ADOBE Photoshop software.

YAC, PAC and cosmid clones

For mapping of the chromosome breakpoints, several YAC clones from a previously established genome-wide YAC panel were used (5). Cosmid clones were selected from a chromosome 19 integrated map (6). Cell culturing, YAC and cosmid DNA isolation was done as described previously (38).

Sequence analysis

Sequences were analysed by BlastN (39) or by the NIX program (40). The RepeatMasker (A.F.H. Smit and P. Green, unpublished data) was used to identify repetitive elements.

Southern blot

Standard methods were employed for the isolation of high molecular weight DNA, restriction, separation and blotting of DNA fragments. Hybridization of labelled fragments was done in the presence of excess salmon sperm competitor DNA. Hybridized filters were washed at 65°C with 40 mM Na_2HPO_4/0.5% SDS for 2 × 30 min. Autoradiography took 16 h at –70°C using two intensifying screens.

Genome walking

A genome walking procedure was performed as described by Siebert *et al.* (41) using *Rsa*I-digested total human DNA. Chromosome 19-specific primers used were rsa, 5′-ATGGGGAGCTGGAACACATC-3′ and rsa(nested), 5′-GGGGCTCTAAAACATCTTTTG-3′. Nested PCR was performed with annealing temperature of 56°C for 30 s and extension for 2 min. The amplification products were cloned into pGEM-T Easy vector (Promega) and double-stranded sequencing was performed with labelled universal M13 primers and the *Taq* dideoxy terminator cycle sequencing kit (Applied Biosystems) on a LI-COR sequencer (MWG-Biotech).

RNA isolation and RT–PCR

Total RNA was isolated from human fibroblast and lymphoblastoid cell lines with the RNeasy Mini Kit (Qiagen). Reverse transcription of total RNA (1 µg) was performed by using either random hexanucleotide priming and Superscript II (Gibco BRL) or the SMART–PCR cDNA synthesis kit (Clontech) according to the provided protocols. In each experiment, DNA contamination was excluded by the absence of a PCR product in the sample without reverse transcriptase amplified under the same conditions as the reverse transcribed RNA sample. To amplify the ORFs of *PAFAH1B3* and *CLK2*, and of the fusion gene *PAFAH1B3Δex5–CLK2Δex1*, nested PCR was performed by using *Pfu* polymerase (Gibco BRL) and the following primers: PAFAH1B3f, 5′-TTTGTTGCCG-CGAGGGGTAG-3′; PAFAH1B3fn, 5′-ACTCGCTCATCCT-GCAGGAG-3′; PAFAH1B3r, 5′-GAGGAAGGAGAGTTTA-ATGTTG-3′; PAFAH1B3rn, 5′-AATGTTGTGGGAAGGC-AGCAG-3′ (*PAFAH1B3*); CLK2f, 5′-GTTGGGGGGGTGG-AGCAGC-3′; CLK2fn, 5′-GTCGCCGCCATCACGGAC-TTC-3′; CLK2r, 5′-CAGGTGAGGGTGGAAACTGTG-3′ and CLK2rn, 5′- GAACTCTGGCTCGTTCTCTTG-3′ (*CLK2*), and PAFAH1B3f, PAFAH1B3fn, CLK2r and CLK2rn (fusion gene). Annealing temperature was 60°C for 30 s and extension for 3 min.

Yeast two-hybrid analysis

The pGBT9-*LIS1* plasmid was constructed by inserting bovine *LIS1* cDNA into the *Eco*RI/*Sal*I sites of the pGBT9 plasmid (Clontech). The resulting plasmid expresses LIS1 as a fusion protein with the DNA binding domain of Gal4. The pGAD424–human *PAFAH1B*3 or pGAD424–human *PAFAH1B3Δex5–CLK2Δex1* plasmids were constructed by inserting the respective cDNA into the *Eco*RI/*Sal*I (human *PAFAH1B3*) or *Bam*HI/*Sal*I (*PAFAH1B3–CLK2*) sites of the pGAD424 plasmid (Clontech). The yeast reporter strain HF7C, which contains the reporter genes *LacZ* and *HIS3* downstream of the binding sequences for Gal4, was sequentially transformed with the pGBT9–*LIS1* plasmid and with the pGAD424–*PAFAH1B3* or pGAD424–*PAFAH1B3Δex5–CLK2Δex1* plasmids using the lithium acetate method. Double transformants were plated on synthetic medium lacking histidine, leucine and tryptophan [(SD)/-Trp/-Leu/-His]. The plates were incubated at 30°C for 3 days. The X-gal colony-lift filter assay for lacZ was performed according to the manufacturer's protocol (Clontech).

Subcellular localization

The *PAFAH1B3Δex5–CLK2Δex1* fusion gene or the murine *Clk2* were subcloned into the vector pEGFP-N1 (Clontech) and the constructs separately transfected into COS-1 cells using FuGENE (Roche). Cell culture has been described previously (11,13) and subcellular localization was analysed by fluorescence microscopy using standard methods.

Splicing assay

The CMV-*Clk1* minigene has been reported previously (13). 293T cells were cotransfected with CMV-*Clk1* and either pEGFPN1–*PAFAH1B3Δex5–CLK2Δex1* or pEGFPN1–*Clk2*. The promotion of exon skipping by either of the two plasmids was analysed by quantitative RT–PCR as described by Duncan *et al.* (13).

ACKNOWLEDGEMENTS

The authors are indebted to Hannelore Madle and Susanne Freier for expert cell culture and chromosome preparations, and Silke Schneider, Sylvia Zacharias and Dietmar Vogt for help with some of the experiments. The German Ressource Centre is gratefully acknowledged for providing genomic libraries and clones. This work was supported by the Bundesministerium für Bildung und Forschung (grant 4763 to H.H.R.).

REFERENCES

1. Chelly, J. (1999) Breakthroughs in molecular and cellular mechanisms underlying X-linked mental retardation. *Hum. Mol. Genet.*, **8**, 1833–1838.
2. Jacobs, P.A. (1974) Correlation between euploid structural chromosome rearrangements and mental subnormality in humans. *Nature*, **249**, 164–165.
3. Jacobs, P.A., Matsura, J.S., Mayer, M. and Newlands, I.M. (1978) A cytogenetic survey of an institution for the mentally retarded: I. Chromosome abnormalities. *Clin. Genet.*, **13**, 37–60.
4. Bühler, E.M. (1983) Unmasking of heterozygosity by inherited balanced translocations. Implications for prenatal diagnosis and gene mapping. *Ann. Genet.*, **26**, 133–137.
5. Wirth, J., Nothwang, H.G., van der, M.S., Menzel, C., Borck, G, Lopez-Pajares, I., Brondum-Nielsen, K., Tommerup, N., Bugge, M., Ropers, H.-H. and Haaf, T. (1999) Systematic characterisation of disease associated balanced chromosome rearrangements by FISH: Cytogenetically and genetically anchored YACs identify microdeletions and candidate regions for mental retardation genes. *J. Med. Genet.*, **36**, 271–278.
6. Ashworth, L.K., Batzer, M.A., Brandriff, B., Branscomb, E., de Jong, P., Garcia, E., Garnes, J.A., Lamerdin, J.E., Lamerdin, J.E., Lennon, G. *et al.* (1995) An integrated metric physical map of human chromosome 19. *Nature Genet.*, **11**, 422–427.
7. Hattori, M., Adachi, H., Tsujimoto, M., Arai, H. and Inoue, K. (1994) The catalytic subunit of bovine brain platelet-activating factor acetylhydrolase is a novel type of serine esterase. *J. Biol. Chem.*, **269**, 23150–23155.
8. Ho, Y.S., Swenson, L., Derewenda, U., Serre, L., Wei, Y., Dauter, Z., Hattori, M., Adachi, T., Aoki, J., Arai, H., Inoue, K. and Derewenda, Z.S. (1997) Brain acetylhydrolase that inactivates platelet-activating factor is a G-protein-like trimer. *Nature*, **385**, 89–93.
9. Winfield, S.L., Tayebi, N., Martin, B.M., Ginns, E.I. and Sidransky, E. (1997) Identification of three additional genes contiguous to the glucocerebrosidase locus on chromosome 1q21: implications for Gaucher disease. *Genome Res.*, **7**, 1020–1026.
10. Hanes, J., von der Kammer, H., Klaudiny, J. and Scheit, K.H. (1994) Characterization by cDNA cloning of two new human protein kinases. Evidence by sequence comparison of a new family of mammalian protein kinases. *J. Mol. Biol.*, **244**, 665–672.
11. Duncan, P.I., Stojdl, D.F., Marius, R.M., Scheit, K.H. and Bell, J.C. (1998) The CLK2 and Clk3 dual-specificity protein kinases regulate the intranuclear distribution of SR proteins and influence pre-mRNA splicing. *Exp. Cell Res.*, **241**, 300–308.
12. Kozak, M. (1987) At least six nucleotides preceding the AUG initiator codon enhance translation in mammalian cells. *J. Mol. Biol.*, **196**, 947–950.
13. Duncan, P.I., Stojdl, D.F., Marius, R.M. and Bell, J.C. (1997) *In vivo* regulation of alternative pre-mRNA splicing by the Clk1 protein kinase. *Mol. Cell. Biol.*, **17**, 5996–6001.
14. Paolella, G., Lucero, M.A., Murphy, M.H. and Baralle, F.E. (1993) The Alu family repeat promoter has a tRNA-like bipartite structure. *EMBO J.*, **2**, 691–696.
15. Hattori, M., Arai, H. and Inoue, K. (1993) Purification and characterization of bovine brain platelet-activating factor acetylhydrolase. *J. Biol. Chem.*, **268**, 18748–18753.
16. Aman, P. (1999) Fusion genes in solid tumors. *Semin. Cancer Biol.*, **9**, 303–318.
17. Albrecht, U., Abu-Issa, R., Ratz, B., Hattori, M., Aoki, J., Arai, H. and Eichele, G. (1996) Platelet-activating factor acetylhydrolase expression and activity suggest a link between neuronal migration and platelet-activating factor. *Dev. Biol.*, **180**, 579–593.
18. Adachi, H., Tsujimoto, M., Hattori, M., Arai, H. and Inoue, K. (1997) Differential tissue distribution of the beta- and gamma-subunits of human cytosolic platelet-activating factor acetylhydrolase (isoform I). *Biochem. Biophys. Res. Commun.*, **233**, 10–13.
19. Reiner, O., Carrozzo R., Shen, Y., Wehnert, M., Faustinella, F., Dobyns, W.B., Caskey, C.T. and Ledbetter, D.H. (1993) Isolation of a Miller-Dieker lissencephaly gene containing G protein beta-subunit-like repeats. *Nature*, **364**, 717–721.
20. Sapir, T., Elbaum, M. and Reiner, O. (1997) Reduction of microtubule catastrophe events by LIS1, platelet-activating factor acetylhydrolase subunit. *EMBO J.*, **16**, 6977–6984.
21. Caspi, M., Atlas, R., Kantor, A., Sapir, T. and Reiner, O. (2000) Interaction between LIS1 and doublecortin, two lissencephaly gene products. *Hum. Mol. Genet.*, **9**, 2205–2213.
22. Faulkner, N.E., Dujardin, D.L., Tai, C.Y., Vaughan, K.T., O'Connell, C.B., Wangs, Y.L. and Vallee, R.B. (2000) A role for the lissencephaly gene LIS1 in mitosis and cytoplasmic dynein function. *Nature Cell Biol.*, **2**, 784–791.
23. Liu, Z., Steward, R. and Lu, L.Q. (2000) *Drosophila* Lis1 is required for neuroblast proliferation, dendritic elaboration and axonal transport. *Nature Cell Biol.*, **2**, 776–783.
24. Smith, D.S., Niethammer, M., Ayala, R., Zhou, Y., Gambello, M.J., Wynshaw-Boris, A. and Tsai, L.H. (2000) Regulation of cytoplasmic dynein behaviour and microtubule organization by mammalian Lis1. *Nature Cell Biol.*, **2**, 767–775.
25. Feng, Y.Y., Olson, E.C., Stukenberg, P.T., Flanagan, L.A., Kirschner, M.W. and Walsh, C.A. (2000) LIS1 regulates CNS lamination by interacting with mNudE, a central component of the centrosome. *Neuron*, **28**, 665–679.
26. Sasaki, S., Shionoya, A., Ishida, M., Gambello, M.J., Yingling, J., Wynshaw-Boris, A. and Hirotsune, S. (2000) A LIS1/NUDEL/cytoplasmic dynein heavy chain complex in the developing and adult nervous system. *Neuron*, **28**, 681–696.
27. Niethammer, M., Smith, D.S., Ayala, R., Peng, J.M., Ko, J., Lee, M.S., Morabito, M. and Tsai, L.H. (2000) NUDEL is a novel Cdk5 substrate that associates with LIS1 and cytoplasmic dynein. *Neuron*, **28**, 697–711.
28. Des Portes, V., Pinard, J.M., Billuart, P., Vinet, M.C., Koulakoff, A., Carrie, A., Gelot, A., Dupuis, E., Motte, J., Berwaldnetter, Y. *et al.* (1998) A novel CNS gene required for neuronal migration and involved in X-linked subcortical laminar heterotopia and lissencephaly syndrome. *Cell*, **92**, 51–61.
29. Gleeson, J.G., Allen, K.M., Fox, J.W., Lamperti, E.D., Berkovic, S., Scheffer, I., Cooper, E.C., Dobyns, W.B., Minnerath, S.R., Ross, M.E. and Walsh, C.A. (1998) Doublecortin, a brain-specific gene mutated in human X-linked lissencephaly and double cortex syndrome, encodes a putative signaling protein. *Cell*, **92**, 63–72.
30. Kornecki, E. and Ehrlich, Y.H. (1988) Neuroregulatory and neuropathological actions of the ether-phospholipid platelet-activating factor. *Science*, **240**, 1792–1794.
31. Clark, G.D., McNeil, R.S., Bix, G.J. and Swann, J.W. (1995) Platelet-activating factor produces neuronal growth cone collapse. *Neuroreport*, **6**, 2569–2575.
32. McNeil, R.S., Swann, J.W., Brinkley, B.R. and Clark, G.D. (1999) Neuronal cytoskeletal alterations evoked by a platelet-activating factor (PAF) analogue. *Cell Mot. Cytoskel.*, **43**, 99–113.
33. Kato, K., Clark, G.D., Bazan, N.G. and Zorumski, C.F. (1994) Platelet-activating factor as a potential retrograde messenger in CA1 hippocampal long-term potentiation. *Nature*, **367**, 175–179.
34. Hill, A.S., Foot, N.J., Chaplin, T.L. and Young, B.D. (2000) The most frequent constitutional translocation in humans, the t(11;22)(q23;q11) is due to a highly specific Alu-mediated recombination. *Hum. Mol. Genet.*, **9**, 1525–1532.
35. Lehrman, M.A., Goldstein, J.L., Russell, D.W. and Brown, M.S. (1987) Duplication of seven exons in LDL receptor gene caused by Alu-Alu recombination in a subject with familial hypercholesterolemia. *Cell*, **48**, 827–835.
36. Stoppa-Lyonnet, D., Duponchel, C., Meo, T., Laurent, J., Carter, P.E., Arala-Chaves, M., Cohen, J.H., Dewald, G.D., Goetz, J., Hauptmann, G. *et al.* (1991) Recombinational biases in the rearranged C1-inhibitor genes of hereditary angioedema patients. *Am. J. Hum. Genet.*, **49**, 1055–1062.

37. Ward, D.C., Boyle, A. and Haaf, T. (1995) Fluorescence in situ hybridization techniques. Metaphase chromosomes, interphase nuclei and extendet chromatin fibers. In Verma, R.S. and Babu, A. (eds), *Human Chromosomes: Principles and Techniques.* MacGraw-Hill, New York, NY, pp. 184–192.
38. Nothwang, H.G., Stubanus, M., Adolphs, J., Hanusch, H., Vossmerbaumer, U., Denich, D., Kubler, M., Mincheva, A., Lichter, P. and Hildebrandt, F. (1998) Construction of a gene map of the nephronophthisis type 1 (Nphp1) region on humanchromosome 2q12-q13. *Genomics*, **47**, 276–285.
39. Altschul, S.F., Madden, T.L., Schäffer, A.A., Zhang, J., Zhang, Z., Miller, W. and Lipman, D.J. (1997) Gapped BLAST and PSI-BLAST: a new generation of protein database search programs. *Nucleic Acids Res.*, **25**, 3389–3402.
40. Williams, G.W., Woollard, P.M. and Hingamp, P. (1998) NIX: a nucleotide identification system at the HGMP-RC. URL: http://www.hgmp.mrc.ac.uk/NIX/.
41. Siebert, P.D., Chenchik, A., Kellogg, D.E., Lukyanov, K.A. and Lukyanov, S.A. (1995) An improved PCR method for walking in uncloned genomic DNA. *Nucleic Acids Res.*, **23**, 1087–1088.
42. Deininger, P.L., Jolly, D.J., Rubin, C.M., Friedmann, T. and Schmid, C.W. (1981) Base sequence studies of 300 nucleotide renatured repeated human DNA clones. *J. Mol. Biol.*, **151**, 17–33.